



Protein Level Defense Responses of *Theobroma cacao* Interaction With *Phytophthora palmivora*

Angra Paula Bomfim Rego¹, Irma Yuliana Mora-Ocampo¹, Carlos Priminho Pirovani¹, Edna Dora Martins Newman Luz^{2†} and Ronan Xavier Corrêa^{1*†}

¹ Department of Biological Sciences, Center of Biotechnology and Genetics, Universidade Estadual de Santa Cruz - UESC, Ilhéus, Brazil, ² Phytopathology Section, Cocoa Research Center, Comissão Executiva do Plano da Lavoura Cacaueira - CEPLAC, Itabuna, Brazil

OPEN ACCESS

Edited by:

Yuxuan Hou,
China National Rice Research
Institute, Chinese Academy of
Agricultural Sciences (CAAS), China

Reviewed by:

Xiao-Ren Chen,
Yangzhou University, China
Kourosh Vahdati,
University of Tehran, Iran

*Correspondence:

Ronan Xavier Corrêa
ronanxc@uesc.br

† These authors share
senior authorship

Specialty section:

This article was submitted to
Disease Management,
a section of the journal
Frontiers in Agronomy

Received: 15 December 2021

Accepted: 18 January 2022

Published: 10 February 2022

Citation:

Rego APB, Mora-Ocampo IY,
Pirovani CP, Luz EDMN and
Corrêa RX (2022) Protein Level
Defense Responses of *Theobroma*
cacao Interaction With *Phytophthora*
palmivora. *Front. Agron.* 4:836360.
doi: 10.3389/fagro.2022.836360

Species of the genus *Phytophthora* cause black-pod rot, which is the disease responsible for the largest losses in cocoa production in the world. The species *Phytophthora palmivora* affects cacao tree cultivation in all producing countries. However, proteomic level studies of the *Theobroma cacao*-*P. palmivora* interaction are incipient. Thus, the aim of this study was to analyze this pathosystem through comparative proteomics and systems biology analyses. The proteins were extracted from leaves of *T. cacao* PA 150 (resistant) and SIC 23 (susceptible) clones 48 h after inoculation with *P. palmivora* using inoculation with sterile distilled water as controls. There were differences in the protein profile between the control and inoculated treatments of both clones. Thirty-seven distinct proteins were identified on 88 spots of the PA 150 treatments, and 39 distinct proteins were identified on 120 spots of the SIC 23 treatments. The metabolisms of ATP, carbohydrates, and nitrogen compounds had higher percentages of proteins with increased accumulation after inoculation in both clones. Systems biology analysis demonstrated that the networks contain a higher number of proteins in the clusters corresponding to processes of photosynthesis and glucose metabolism, suggesting that they are the most affected by the infection. In addition, lipoxygenase (LOX), 2-methylene-furan-3-one reductase-like, and co-chaperonin CPN20 proteins and a probable CC-NBS-LRR protein may be involved in resistance to black-pod disease caused by *P. palmivora*.

Keywords: black-pod disease, Oomycete, genetics, phytopathology, plant improvement, plant-pathogen interaction, proteomics, systems biology

INTRODUCTION

Theobroma cacao L. beans are the raw material for chocolate production, with an international trade valued at US \$103 billion per year. However, losses caused by diseases affect up to 38% of the annual global cocoa harvest (Marelli et al., 2019). The most economically important cocoa tree disease black-pod rot is caused by *Phytophthora* species that infect the fruits, being responsible for the loss of 20–25% of cocoa production, which is approximately 700,000 metric tons on a global scale (Adeniyi, 2019). *Phytophthora megakarya* (Brasier and Griffin) occurs only in countries of West and Central Africa and is considered a significant pathogen only in cacao, whereas *Phytophthora palmivora* (E. J. Butler) is present in all cocoa producing countries and has a wide range of hosts (Ali et al., 2017; Perrine-Walker, 2020).

Phytophthora palmivora is a hemibiotrophic Oomycete capable of infecting more than 200 species of plants (Perrine-Walker, 2020) with the capacity to infect leaves, branches, fruits, stalk, and roots. The symptoms appear in infected fruits around 4 days after penetration of the germ tube in the mesocarp and in the biotrophic phase establishment. During the necrotrophic phase, secondary hyphae kill the host cell, a brown lesion develops, and the fruit is no longer suitable for harvesting (Bowers et al., 2001; Perrine-Walker, 2020).

Black-pod rot can be controlled using cultivation practices such as removal of infected fruits and pods and phytosanitary pruning of the cacao tree, associated with chemical, genetic, and biological methods to ensure integrated disease control management in cocoa tree plantations (Macagnan et al., 2006; Zhang and Motilal, 2016). The use of resistant varieties is a more effective alternative for disease control (Barreto et al., 2015), although many cocoa cultivars are susceptible to this disease.

Studies on the *Phytophthora-T.cacao* interaction have focused on anatomic/histological differences, enzymes, genes, and metabolites of varying influence on resistance to black-pod rot (Bailey et al., 2016; Gu et al., 2020). However, there are few studies specifically on the *P. palmivora-T.cacao* interaction. One such study evaluated 262 cacao genotypes regarding genetic resistance and it was found that resistance to black-pod rot is polygenic in cross-breeds involving resistant and susceptible genotypes (Dantas Neto et al., 2005) and oligogenic in cultivars of average resistance (Barreto et al., 2015). In a transcriptomic analysis, the expression of 5,264 cocoa genes was altered after *P. palmivora* infection, including subsets of genes involved in biosynthesis of phenylpropanoid, biosynthesis and action of ethylene and jasmonic acid (JA), plant defense signal transduction, and endocytosis, which were induced in response to infection (Ali et al., 2017). Furthermore, a large subset of genes that codify putative proteins related to pathogenesis (PR) also showed differential expression in response to infection (Ali et al., 2017).

However, biological issues can only be addressed at protein level due to different levels of genic regulation and post-translational modifications (Quirino et al., 2010). This type of analysis provides information on the molecular mechanisms of resistance in plants (Geddes et al., 2008).

Some aspects of the *T. cacao-Moniliophthora perniciosa* pathosystem have already been addressed through proteomic analysis (Almeida et al., 2017; dos Santos et al., 2020; Mares et al., 2020). Proteins from the leaf water wash (LWW) of CCN51 genotype were analyzed by 2D-SDS/PAGE followed by tandem mass spectrometry, and 42 proteins (28 from the cocoa and 14 from bacteria) were identified, including proteins related to defense and synthesis of defense metabolites and involved in nucleic acid metabolism (Almeida et al., 2017). The changes in protein expression in basidiospores of the fungus *M. perniciosa* in response to the LWW of two contrasting cacao varieties for resistance to witches' broom disease were described in a proteomic analyses (Mares et al., 2020). The proteomic analysis was performed by the 2D-PAGE technique combined with mass spectrometry (MS) revealed proteins associated with energy (ATP synthase) and protein (BiP) metabolism, whose accumulation was reduced by basidiospores germinated in leaf wash from "Catongo" cacao. Furthermore, proteins involved

in virulence were identified along with fungal resistance to polyketide cyclase, glycoside hydrolase, multidrug transporter protein (SFM), and proteins related to oxidative stress and fermentation, such as catalase A and alcohol dehydrogenase (ADH) (Mares et al., 2020). On the other hand, in a 2D gel-based approach followed by MS analysis comparing the response of contrasting cacao genotypes for resistance to *M. perniciosa*, the resistant genotype showed expressed proteins associated with stress and defense, while the susceptible genotype pathogenesis related proteins (PRs), oxidative stress regulation related proteins, and trypsin inhibitors were repressed (dos Santos et al., 2020). Nevertheless, despite the large economic impact caused by black pod rot, protein level studies of the response of *T. cacao* to infection by *P. palmivora* are incipient. Thus, this study aims to analyze the *P. palmivora-T. cacao* interaction through a comparative proteomic and systems biology approach, using *T. cacao* PA 150 (resistant) and SIC 23 (susceptible) clones inoculated with *P. palmivora* to uncover the possible defense mechanisms of the plant.

MATERIALS AND METHODS

Plant Material and Inoculation in Leaf Discs

Fully expanded and physiologically mature leaves from *T. cacao* clones PA 150, resistant, and SIC 23 susceptible to black-pod rot were collected from plants of the active germplasm bank of the Cacao Research Center—CEPEC/Executive Commission of the Cacao Tree Plantation Plan—CEPLAC. So, 10 adult 20-year-old plants were used to obtain leaves from each cacao clone. The *P. palmivora* isolate was obtained from the culture collection Arnaldo Medeiros of the CEPEC (Luz et al., 2008). The inoculations were performed on leaf discs according to the methodology developed by Nyassé et al. (1995), with modifications to the aliquot volume to 20 μ l of the zoospore suspension of *P. palmivora* at a concentration of 3×10^5 zoospores/ml.

Total Protein Extraction From Cacao Leaf

The total protein extracts from leaves of the control and inoculated treatments after 48 h were obtained using phenol extraction followed by precipitation with ammonium acetate 0.1 mol L⁻¹ in methanol, as described by Pirovani et al. (2008). A total of 1.0 g of leaf tissue, previously macerated in liquid nitrogen and in the presence of polyvinylpyrrolidone antioxidant (PVPP), was used for each treatment, using a procedure based on successive washes, associated with steps of sonication. In the second extraction stage, phenols and dense SDS were used. The precipitated proteins were resuspended in rehydration buffer, composed by 8 mol L⁻¹ urea, 2% chaps, 2% IPG buffer 3–10, bromophenol blue 0.002%. The proteins were quantified using 2D-Quant (GE HealthCare) kit, following the manufacturer's instructions.

Electrophoresis in the First and Second Dimension

First dimension electrophoresis was carried out in strips in the non-linear (NL) 3–10 pH band (Amersham Biosciences, Immobiline Dry-Strip). Total protein (500 μ g) was homogenized

in rehydration buffer containing Dithiothreitol (DTT), at a concentration of 50 mmol L⁻¹ and 0.5% ampholytes, totaling 250 µl. The strips were focalized using EttanIPGhor3 (GE Healthcare) equipment, with Ettan IPGhor3 software, in accordance with a rehydration time of 12 h at 20°C and running conditions of 500 Vh for 1 h, 1,000 Vh for 1 h 04, 8,000 Vh for 2 h 30, and 8,000 Vh for 40 min. After isoelectric focalization of the strips, they were incubated for 15 min with equilibrium buffer (Urea at 6 M, Tris-HCl (75 mmol L⁻¹, pH 8.8), glycerol at 30%, SDS at 2%, and bromophenol blue at 0.002%), containing DTT 10 mg ml⁻¹; for a further 15-min period in iodoacetamide at 25 mg ml⁻¹ (Buffer Tris-HCl 50 mM, pH 8.8, urea 6 M, glycerol at 30%, SDS at 2%, iodoacetamide at 1%, trace of bromophenol blue); and, finally, for 15 more min in running buffer 1X (Tris at 0.25 mol L⁻¹, glycine at 1.92 mol L⁻¹, SDS at 1%, pH 8.5). The strips were placed on vertical SDS-PAGE gel at 12.5%. The second dimension (2-DE) was carried out on a Ruby SE600 (GE Healthcare) system: 15 mA/gel for 15 min, 40 mA/gel for 30 min, and, finally, 50 mA/gel for 5 h, for each strip, at a constant temperature of 11°C. All the 2-D gel separations were repeated three times for each treatment. After electrophoresis, the proteins were visualized with 0.08% Coomassie Blue G-250 (Neuhoff et al., 1988). The gels were colored and discolored for 7 days under constant agitation. After this period, the gels were maintained in acetic acid at 7%. The gel images were obtained through a LabScanner (Amersham Bioscience) and analyzed using Image Master 2D Platinum 7.0 software (GE Healthcare). The gels were reproduced in triplicate for each sample in order to increase reproducibility of the analysis. The control samples were compared to samples inoculated with *P. palmivora* for each cacao clone. The analysis of spots differentially accumulated between the variety of treatments was based on ANOVA calculation, where values of $p \leq 0.05$ and spots with variations of intensity (fold) >1.5 were considered (**Supplementary Tables 1, 2**).

Mass Spectrometry

The spots of interest were excised from 2-DE gel using a scalpel and proteolytic digestion was carried out according to Shevchenko et al. (2007). The solution containing the proteolytic was fragmented through reverse phase chromatography in a nanoAcquity UPLC (WATERS) attached to the Q-ToF micro mass spectrometer (Waters), as per Silva et al. (2013). The obtained spectra were analyzed using ProteinLynx v2.3 software and compared with the *T. cacao* genome database of NCBI, using the MASCOT MS/MS IonSearch tool (www.matrixscience.com; **Supplementary Tables 3, 4**; Argout et al., 2008). The criteria used for research were trypsin enzyme digestion, carbamidomethyl (Cys) with fixed modification, and oxidation (Met), as variable modification; a maximum of one loss of the cleavage site; and ± 0.3 Da for the peptide tolerance error and 0.1 Da for fragmented ions error (Silva et al., 2013; Villela-Dias et al., 2014). The generated FASTA sequences were analyzed using Blast2GO software (<http://www.blast2go.com>), which provides important information, such as ontology, functions, biological processes, and cellular localization.

Systems Biology

To obtain information on the protein–protein interactions based on the proteomic profiles of *T. cacao*, homologous proteins in *Arabidopsis thaliana* were sought out. To achieve this objective, all the identified proteins with their FASTA sequences were processed using STRING 11.0 (<http://string-db.org>) software. The proteins were individually analyzed with the following parameters: meaning of network edges: confidence; active interaction sources: textmining, experiments, databases, co-expression, neighborhood, gene fusion, and co-occurrence; minimum required interaction score: high confidence (0.700) more than 50 interactions, significance level of 0.7; max number of interactors to show: first and second shell: no more than 50 interactions. The file for each network was downloaded in TSV format and the files were subsequently merged and analyzed using Cytoscape software version 3.7.1. The properties of modularity and centrality (betweenness and node degree; **Supplementary Tables 5, 6**) of the network were calculated through the igraph package of the RStudio statistical tool (RStudio Team, 2019). An analysis of genic ontology enrichment was carried out for each cluster (**Supplementary Tables 7, 8**) through the BiNGO plugin version 3.0.3 (Shannon, 2003).

RESULTS

Proteomic Analyses

There were differences in the protein profile between the treatment inoculated with *P. palmivora* zoospores and the control treatment (placebo), both for clone PA 150 (resistant) and for clone SIC 23 (susceptible) (**Figure 1**). A total of 392 spots were identified in the inoculated treatment of the clone PA 150, whereas 326 spots were identified in the control treatment. Of these, 143 were identified exclusively in the inoculated treatment and 77 exclusively in the control treatment, while 249 spots were common to both treatments. Of these, 30 were differentially accumulated (fold >1.5; 0.05 ANOVA).

In turn, 300 spots were identified in the inoculated treatment of the clone SIC 23, and 346 spots were identified in the control treatment. Of these, 78 were identified exclusively in the inoculated treatment and 124 were detected exclusively in the control treatment, while 222 spots were common to both treatments. Among the spots in common, 31 were differentially accumulated (fold >1.5; $p < 0.05$ ANOVA).

Finally, 37 distinct proteins were identified on 88 spots of the PA 150 treatments (**Table 1**) and 39 distinct proteins were identified on 120 spots of the SIC 23 treatments (**Table 2**).

The identified proteins were organized into 10 biological processes (**Figure 2**). It was observed that some proteins belonged to more than one process (**Tables 1, 2**). The graph in **Figure 2** shows the percentage of proteins that had reduced or increased accumulation, in each process, at 48 hai in the PA 150 (**Figure 2A**) and SIC 23 (**Figure 2B**) clones. Proteins identified on more than one spot with different accumulation were added both to up-accumulated and down-accumulated proteins.

In the resistant genotype (**Figure 2A**), the processes that had a higher percentage of proteins with increased accumulation

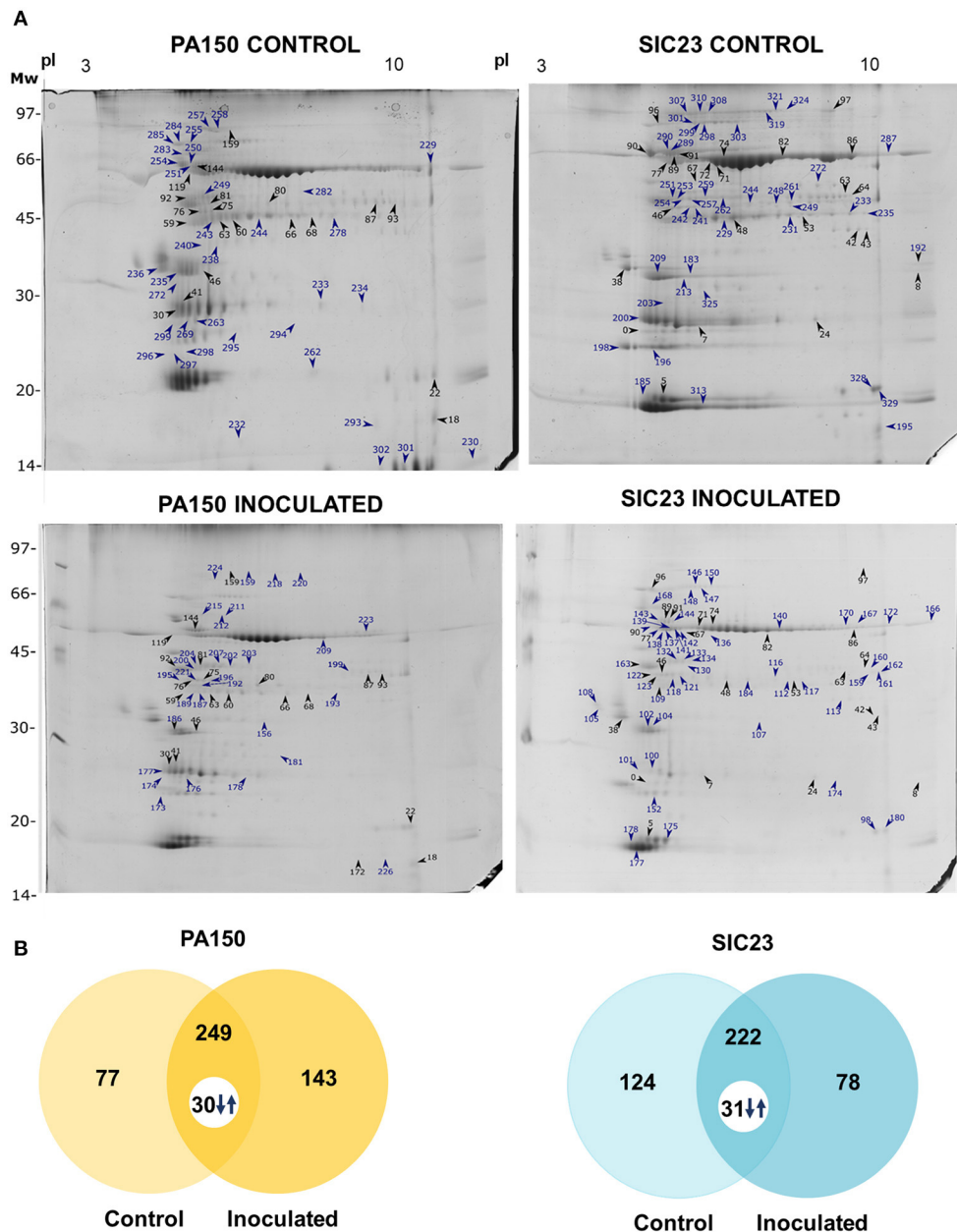


FIGURE 1 | Electrophoretic profiles of cacao leaves inoculated and not inoculated with *P. palmivora*. **(A)** SDS-PAGE-2D representative of the inoculated and control treatments of each clone. The spots marked with arrows and numbers are those from which the proteins in **Tables 1, 2** were identified. Blue arrows and numbers indicate the spots detected exclusively in each treatment; black arrows and numbers indicate common spots that are differentially accumulated; **(B)** Venn diagrams representing the spots detected in resistant (PA 150) and susceptible (SIC 23) clones in the control and inoculated treatments. The numbers accompanied by arrows are the spots common to both treatments that had a significant difference in accumulation considering the ANOVA $p < 0.05$ and fold > 1.5 parameters.

after inoculation with *P. palmivora* were the metabolic process of ATP, the oxide-reduction process, photosynthesis, and the metabolic process of carbohydrates and nitrogen compounds. On the other hand, the processes that had a higher percentage of proteins with reduced accumulation during infection were defense or response to stress or stimulus, protein folding, other processes, and not noted. The metabolic process of proteins was maintained at the

same percentage of proteins with increased accumulation and reduced accumulation.

In the susceptible clone (**Figure 2B**), the processes that had a higher percentage of proteins with increased accumulation at 48 hai were protein folding, the metabolic process of ATP, and nitrogen compound metabolism. Those that had a higher percentage of proteins with reduced accumulation were the oxide-reduction process,

photosynthesis, other processes, and not noted. However, the processes of defense or response to the stimulus, protein metabolism, and carbohydrate metabolism maintained the same percentage.

Protein Interaction Networks

The interaction network corresponds to the homologous proteins identified in the PA 150 (**Figure 3A**) clone resulting in 1,339 knots, 28,131 connectors, and 14 clusters, to which biological functions were attributed, such as response to wounds, lipid transport, photosynthesis, biosynthesis of cuticular hydrocarbons, and protein folding, among others (**Supplementary Table 7**). In the same network, there was a total of 177 bottleneck proteins and 515 protein hubs (**Supplementary Table 5**).

In turn, the network corresponding to the proteins homologous to those identified in the SIC 23 clone (**Figure 3B**) presented a total of 1,466 knots, 27,198 connectors, and 15 clusters, which corresponded to biological functions such as response to stress, microtubule-based process, and photosynthesis, among others (**Supplementary Table 8**). In this network, 201 proteins were bottleneck and there were 573 hubs (**Supplementary Table 6**).

DISCUSSION

The black-pod rot disease, caused by species of the genus *Phytophthora*, is responsible for great losses in global cacao production. Here, responses of two contrasting clones for *P. palmivora* resistance were compared at proteomic level. Proteins related to photosynthesis, glucose metabolism, response to stress and oxidation–reduction process were identified (**Figure 1**). Through the different patterns of protein accumulation, differences in molecular responses between susceptible and resistant genotypes were elucidated, such as declining cellular energy, balance in the production and detoxification of ROS, control of cytotoxic metabolites, production of JA, and participation of a protein encoded by a resistance gene (R).

Decreased RCA Accumulation in the Susceptible Clone Could Lead to Energy Decline in the Cell

Ribulose biphosphate carboxylase/oxygenase (rubisco) protein, was identified on seven spots in the PA 150 clone (**Table 1**); four with reduced accumulation (spots 172, 230, 301, and 302) and three with increased accumulation (spots 159, 209, and 226). In turn, the same protein was identified on 12 spots in the SIC 23 clone (**Table 2**); eight with increased accumulation (spots 74, 82, 86, 90, 140, 166, 170, and 172) and four with reduced accumulation (spots 71, 72, 251, and 287). This protein is one of the main enzymes in the second phase of photosynthesis. Interestingly, RuBisCO Activase (RCA), which is required for rubisco to function properly, showed reduced accumulation in the susceptible clone (spots 253, 254, and 259) and increased accumulation in PA 150 (spot 200). However, it required ATP

to perform its activase function (Portis et al., 2007; Carmo-Silva and Salvucci, 2011). Thus, six spots corresponding to ATP synthase subunits were identified in the resistant clone, of which three showed an increased accumulation (**Table 1**; spots 144, 189, and 221) and three showed reduced accumulation (spots 119, 250, and 232), whereas the susceptible clone had 14 spots identified as corresponding to ATP synthase subunits, of which 13 had increased accumulation (**Table 2**; spots 46, 77, 89, 91, 121, 137–139, 141–144, and 167).

Therefore, in the susceptible clone, where RCA had reduced accumulation, there was a higher number of spots corresponding to rubisco and ATPase with increased accumulation, in contrast to the resistant clone. As a result, we can propose the following scenario: a decrease in the quantity of RCA in the SIC 23 clone resulted in deficient rubisco activity, which leads to an imbalance in the Calvin cycle, and, as a consequence, a decrease in sugars production in the cell. As a result, energy production would be reduced. Thus, there should have been cellular compensation for the energy loss, with increased expression of rubisco and ATP synthase.

RuBisCO Activase is one of the most important proteins within the interaction network related to homologous proteins identified in both clones (**Figure 3**) since its values of betweenness and node degree are close to the maximum values (**Supplementary Tables 5, 6**). Therefore, it is considered a protein with an important role in regulation and signaling within the organism (Verli, 2014).

Balance in the ROS Production and Detoxification in the Resistant Clone

The photosystems I and II subunits were identified on different spots (**Tables 1, 2; Figure 2**), which had different accumulation in both clones 48 hai. It is well-known that these reaction centers are the primary source of reactive oxygen species (ROS) (Asada, 2006); a decrease in photosystem expression causes an increase in ROS production (Oukarroum et al., 2015). Thus, the different expression patterns of the subunits of PSI and PSDII observed in the PA 150 and SIC 23 clones may be involved in varying levels of ROS production.

Furthermore, it was observed that the chlorophyll a-b binding protein, also called light-harvesting chlorophyll a/b-binding (LHCB), had reduced accumulation in both clones (**Table 1**, spot 263; **Table 2**, spots 0, 200, and 203). This protein absorbs solar light and drives the transport of photosynthetic electrons (Jansson, 1994; Liu et al., 2013). Moreover, LHCBs are positively involved in ABA signaling by modulating ROS homeostasis (Xu et al., 2012). Therefore, a decrease in the expression of LHCB protein in both clones suggests a decrease in the ABA pathway, promoting the accumulation of H₂O₂ (Asselbergh et al., 2008). In that regard, the co-chaperonin CPN20 was identified in the PA 150 clone as exclusive (spot 176). This protein negatively regulates the signaling of ABA (Zhang et al., 2013), reinforcing the theory that ABA pathway is repressed, and is responsible for the activation of iron superoxide dismutase (FeSODs; FSDs) enzymes, whose function is to dismutase superoxide (O⁻) in H₂O₂ (Kuo et al., 2013a,b).

TABLE 1 | Proteins identified through mass spectrometry in leaves of the PA 150 resistant clone of *T. cacao* inoculated and not inoculated with *P. palmivora*.

N° Spot ^a	N° Acesso	Nome da proteína e organismo referência	MM ^b	pI ^c	Score ^d	Fold ^e	Proc. Biol. ^f
18	EOY30176.1	Thioredoxin superfamily protein, Q [<i>Theobroma cacao</i>]	23,284	9.60	219	2,3	OR/DR
22	XP_007034724.1	Photosystem I reaction center subunit II, chloroplastic [<i>Theobroma cacao</i>]	23,982	9.38	213	1,5	P
30	XP_008787626.1	DNA ligase 6-like [<i>Phoenix dactylifera</i>]	1,582,226	6.94	54	2,7	DR
41	EOY19427.1	Cc-nbs-lrr resistance protein, putative [<i>Theobroma cacao</i>]	309,414	5.19	432	−2	DR
46	EOX9125.1	Photosystem II subunit O-2 [<i>Theobroma cacao</i>]	35,364	5.20	906	2,9	P
59	EOY17906.1	Sedoheptulose-bisphosphatase [<i>Theobroma cacao</i>]	42,692	6.56	577	2,7	C
60	BAC10972.1	Fructose-bisphosphate aldolase [<i>Physcomitrella patens</i>]	14,922	7.60	55	−1,7	C
63	KHN00649.1	Glyceraldehyde-3-phosphate dehydrogenase A, chloroplastic [<i>Glycine sojae</i>]	31,034	9.71	56	−2,4	C
66	EOX97859.1	Fructose-bisphosphate aldolase 1 [<i>Theobroma cacao</i>]	43,279	8.43	250	−1,5	C
68	X_P007032095.1	Glyceraldehyde-3-phosphate dehydrogenase A, chloroplastic [<i>Theobroma cacao</i>]	43,255	8.15	539	1,6	C
75	P27774.1	Glyceraldehyde-3-phosphate dehydrogenase A, chloroplastic [<i>Theobroma cacao</i>]	43,255	8.15	397	2	C
76	XP_007040771.1	Phosphoribulokinase, chloroplastic [<i>Theobroma cacao</i>]	44,486	6.03	84	1,6	NC/C/P
80	XP_008787626.1	DNA ligase 6-like [<i>Phoenix dactylifera</i>]	158,222	6.94	54	2,9	DR
81	XP_008787626.1	DNA ligase 6-like [<i>Phoenix dactylifera</i>]	158,222	6.94	54	2,4	DR
87	XP_008787626.1	DNA ligase 6-like [<i>Phoenix dactylifera</i>]	158,222	6.94	54	1,8	DR
92	XP_008787626.1	DNA ligase 6-like [<i>Phoenix dactylifera</i>]	158,222	6.94	54	3,3	DR
93	XP_007026120.1	Aminomethyltransferase, mitochondrial [<i>Theobroma cacao</i>]	44,708	6.92	135	−3,3	NC
119	AAD00593.2	ATP synthase beta subunit, partial (chloroplast) [<i>Glaucium flavum</i>]	51,055	5.09	147	−5,3	ATP
144	AMC30632.1	ATP synthase CF1 alpha subunit (chloroplast) [<i>Callitriche involucrata</i>]	55,437	5.2	510	3,2	ATP
156	EOY17906.1	Sedoheptulose-bisphosphatase [<i>Theobroma cacao</i>]	42,692	6.56	328	∞	C
159	EOY19427.1	Cc-nbs-lrr resistance protein, putative [<i>Theobroma cacao</i>]	309,414	5.19	159	4,5	DR
159	CAB00001.1	RuBisCO [<i>Calophyllum</i> sp.]	52,268	5.96	60	∞	P
172	XP_007033270.1	RuBisCO small chain, chloroplastic [<i>Theobroma cacao</i>]	21,174	9.22	493	0	P
173	EOX93083.1	Photosystem II subunit P-1 [<i>Theobroma cacao</i>]	28,666	8.65	276	∞	P
174	NP_001137046.1	2-cys peroxyredoxine BAS1 [<i>Zea mays</i>]	28,236	6.18	326	∞	OR/DR
176	EOY30200.1	Chaperonin 20 isoform 2 [<i>Theobroma cacao</i>]	26,752	8.55	252	∞	PF/DR
177	EOY21247.1	Putative 21 kDa Trypsin Inhibitor [<i>Theobroma bicolor</i>]	24,264	5.71	486	∞	PM
178	EOY19427.1	Cc-nbs-lrr resistance protein, putative [<i>Theobroma cacao</i>]	309,414	5.19	433	∞	DR
181	EOY18135.1	Triosephosphate isomerase isoform 1 [<i>Theobroma cacao</i>]	32,446	8.05	80	∞	NC/C
186	EOX91250.1	Photosystem II subunit O-2 [<i>Theobroma cacao</i>]	35,364	5.85	798	∞	P
187	P09043.1	Phosphoribulokinase, chloroplastic [<i>Theobroma cacao</i>]	42,122	6.60	139	∞	NC/C/P
189	XP_007026083.1	ATP synthase gamma chain, chloroplastic [<i>Theobroma cacao</i>]	41,685	5.57	359	∞	ATP
192	XP_013445984.1	2-methylene-furan-3-one reductase-like [<i>Medicago truncatula</i>]	41,030	7.64	187	∞	OR/NC
193	EOY02669.1	Glyceraldehyde-3-phosphate dehydrogenase C2 isoform 1 [<i>Theobroma cacao</i>]	35,816	8.51	194	∞	C
195	EOY21247.1	Putative 21 kDa Trypsin Inhibitor [<i>Theobroma bicolor</i>]	24,264	5.71	252	∞	PM
196	P27774.1	Phosphoribulokinase, chloroplastic [<i>Theobroma cacao</i>]	44,486	6.03	83	∞	NC/C/P
199	XP_007026120.1	Aminomethyltransferase, mitochondrial [<i>Theobroma cacao</i>]	44,708	8.86	97	∞	NC
200	XP_007009267.1	RuBisCO activase isoform X2 [<i>Theobroma cacao</i>]	48,566	5.56	580	∞	DR
202	CDP01929.1	fructose-bisphosphate aldolase chloroplastic [<i>Coffea canephora</i>]	35,264	8.76	71	∞	C
203	EOY15330.1	Glyceraldehyde-3-phosphate dehydrogenase B subunit [<i>Theobroma cacao</i>]	48,483	6.76	90	∞	C
204	XP_017980600.1	Phosphoglycerate kinase, chloroplastic [<i>Theobroma cacao</i>]	51,447	8.49	492	∞	NC/C
207	XP_017973236.1	Elongation factor Tu, chloroplastic [<i>Theobroma cacao</i>]	52,371	6.45	269	∞	PM
209	AGD79694.1	RuBisCO [<i>Brosimum Guyanense</i>]	51,328	7.0	507	∞	Ph
211	EOY19427.1	Cc-nbs-lrr resistance protein, putative [<i>Theobroma cacao</i>]	309,414	5.19	96	∞	DR
212	EOY19427.1	Cc-nbs-lrr resistance protein, putative [<i>Theobroma cacao</i>]	309,414	5.19	751	∞	DR
215	EOY19427.1	Cc-nbs-lrr resistance protein, putative [<i>Theobroma cacao</i>]	309,414	5.19	685	∞	DR
218	EOY29899.1	Glycine decarboxylase P-protein 1 [<i>Theobroma cacao</i>]	114,581	6.88	92	∞	NC/OR
220	XP_008787626.1	DNA ligase 6-like [<i>Phoenix dactylifera</i>]	158,222	6.94	54	∞	DR
221	ADO64897.2	ATP synthase CF1 beta subunit (chloroplast) [<i>Theobroma cacao</i>]	53,689	5.29	1,503	∞	ATP
223	EOX91867.1	Serine trans hydroxymethyltransferase 1 isoform 2 [<i>Theobroma cacao</i>]	47,274	9.01	528	∞	NC
224	EOY32513.1	Lipoxygenase isoform 1 [<i>Theobroma cacao</i>]	103,618	5.74	555	∞	OR

(Continued)

TABLE 1 | Continued

N° Spot ^a	N° Acesso	Nome da proteína e organismo referência	MM ^b	pI ^c	Score ^d	Fold ^e	Proc. Biol. ^f
226	XP_007033270.1	RuBisCO small chain, chloroplastic [<i>Theobroma cacao</i>]	21,174	9.22	474	∞	Ph
229	XP_007009760.1	Elongation factor 1-alpha [<i>Theobroma cacao</i>]	49,819	9.15	336	0	PM
230	EOY04195.1	RuBisCO (small chain) family protein isoform 1 [<i>Theobroma cacao</i>]	21,647	9.22	340	0	Ph
232	ABN08803.1	ATPase, alpha/beta subunit [<i>Medicago truncatula</i>]	66,712	5.71	71	0	ATP
233	OAY79436.1	Uncharacterized protein [<i>Ananas comosus</i>]	34,588	8.59	56	0	Un
234	EOY02403.1	Carbonic anhydrase 1 isoform 2 [<i>Theobroma cacao</i>]	35,284	8.35	308	0	OP
235	EOX91250.1	Photosystem II subunit O-2 [<i>Theobroma cacao</i>]	35,364	5.85	870	0	Ph
236	XP_017985371	60 kDa jasmonate-induced -like [<i>Theobroma cacao</i>]	54,475	4.84	751	0	DR
238	OAY60877.1	Ferredoxin–NADP leaf chloroplastic [<i>Manihot esculenta</i>]	40,846	8.79	248	0	OR
240	OAY60877.1	Ferredoxin–NADP leaf chloroplastic [<i>Manihot esculenta</i>]	40,846	6.79	255	0	OR
243	EOX97859.1	Fructose-bisphosphate aldolase 1 [<i>Theobroma cacao</i>]	43,279	8.43	622	0	C
244	EOX97859.1	Fructose-bisphosphate aldolase 1 [<i>Theobroma cacao</i>]	43,279	8.43	211	0	C
249	EOY15330.1	Glyceraldehyde-3-phosphate dehydrogenase B subunit [<i>Theobroma cacao</i>]	48,483	6.76	483	0	C
250	Q9MRF3.1	ATP synthase subunit beta, chloroplastic [<i>Theobroma cacao</i>]	53,654	5.43	517	0	ATP
251	EOY19427.1	Cc-nbs-lrr resistance protein, putative [<i>Theobroma cacao</i>]	309,414	5.19	81	0	DR
254	XP_017985371.1	60 kDa jasmonate-induced -like [<i>Theobroma cacao</i>]	54,475	4.84	779	0	DR
255	CDP00073.1	heat shock cognate 70 kDa 2-like [<i>Coffea canephora</i>]	70,139	5.22	57	0	PF/DR
257	XP_00878762.1	DNA ligase 6-like [<i>Phoenix dactylifera</i>]	158,222	6.94	54	0	DR
258	XP_008787626.1	DNA ligase 6-like [<i>Phoenix dactylifera</i>]	158,222	6.94	54	0	DR
262	AAL85660.1	Trypsin inhibitor, partial [<i>Theobroma sylvestri</i>]	16,845	4.64	241	0	PM
263	XP_007021260.2	Chlorophyll a-b binding protein 3, chloroplastic [<i>Theobroma cacao</i>]	28,741	5.65	272	0	Ph
269	EOY02403.1	Carbonic anhydrase 1 isoform 2 [<i>Theobroma cacao</i>]	35,284	4.82	748	0	OP
272	EOX91250.1	Photosystem II subunit O-2 [<i>Theobroma cacao</i>]	35,364	5.85	560	0	Ph
278	XP_008787626.1	DNA ligase 6-like [<i>Phoenix dactylifera</i>]	158,222	6.94	54	0	DR
282	XP_008787626.1	DNA ligase 6-like [<i>Phoenix dactylifera</i>]	158,222	6.94	54	0	DR
283	EOY32236.1	TCP-1/cpn60 chaperonin family protein [<i>Theobroma cacao</i>]	64,513	5.62	360	0	PF/DR
284	CDP00073.1	Heat shock cognate 70 kDa 2-like [<i>Coffea canephora</i>]	705,139	5.22	58	0	PF/DR
285	XP_008787626.1	DNA ligase 6-like [<i>Phoenix dactylifera</i>]	158,222	6.94	54	0	DR
293	Q5S1S6.1	Peroxiredoxin Q, chloroplastic [<i>Theobroma cacao</i>]	23,691	9.72	70	0	OR/DR
294	EOY30280.1	auxin-binding ABP19a-like [<i>Theobroma cacao</i>]	29,756	9.46	129	0	DR
295	EOX93083.1	Photosystem II subunit P-1 [<i>Theobroma cacao</i>]	28,666	8.65	325	0	Ph
296	XP_008787626.1	DNA ligase 6-like [<i>Phoenix dactylifera</i>]	158,222	6.94	54	0	DR
297	EOY21247.1	Putative 21 kDa Trypsin Inhibitor [<i>Theobroma bicolor</i>]	24,264	5.71	252	0	PM
298	EOY21251.1	Putative 21 kDa Trypsin Inhibitor [<i>Theobroma bicolor</i>]	24,263	5.94	450	0	PM
299	NP_001304217.1	2-Cys peroxyredoxin BAS1, chloroplastic type [<i>Vigna radiata</i>]	22,098	4.86	300	0	OR/DR
301	EOY04195.1	RuBisCO (small chain) family protein isoform 1 [<i>Theobroma cacao</i>]	21,647	9.22	245	0	Ph
302	EOY04195.1	RuBisCO (small chain) family protein isoform 1 [<i>Theobroma cacao</i>]	21,647	9.22	118	0	Ph

^aSpot number assigned in the analysis of gels using ImageMaster 2D Platinum 7.0 software, as indicated in Figure 1B.

^bTheoretical molecular weight in Daltons assigned by MASCOT.

^cTheoretical Isoelectric Point assigned by MASCOT.

^dScore assigned by MASCOT, being the sum of the highest score of ions for each distinct sequence.

^eFold corresponds to the alteration in expression between inoculated and control treatments, calculated using ImageMaster 2D Platinum 7.0 software: (0) identified exclusively in the control treatment, (∞) identified exclusively in the inoculated treatment, (+) super accumulated in the inoculated treatment, (–) super accumulated in the control treatment.

^fBiological process to which the protein belongs according to the Blast2GO tool and the Uniprot database: ATP, metabolism of ATP; Ph, photosynthesis; DR, defense/response to stress/stimulus; PF, protein folding; PM, protein metabolism; OR, oxide-reduction process; C, carbohydrate metabolism; NC, nitrogen compound metabolism; OP, other processes; Un, not noted.

Moreover, a 2-cys peroxyredoxine BAS1, an enzyme involved in the regulation of plastidial H₂O₂ concentration (Awad et al., 2015), was exclusively identified in the PA 150 clone (Table 1; spot 174). A 2-cys peroxyredoxine was also identified with

increased accumulation in the resistant clone of the pathosystem *T. cacao*–*M. pernicioso* (dos Santos et al., 2020). This evidence suggests that there is a more efficient ROS production and detoxification system against infection with *P. palmivora*.

TABLE 2 | Proteins identified through mass spectrometry in leaves of the SIC 23 susceptible clone of *T. cacao* inoculated and not inoculated with *P. palmivora*.

N° Spot ^a	N° Acesso	Nome da proteína e organismo referência	MM ^b	pI ^c	Score ^d	Fold ^e	Proc. Biol. ^f
0	EOY12785.1	PREDICTED: chlorophyll a-b binding protein 13 [<i>Gossypium hirsutum</i>]	28,713	5.65	69	−3,2	P/DR
5	AAV41233.1	Putative 21 kDa Trypsin Inhibitor [<i>Theobroma bicolor</i>]	24,264	5.71	782	2	PM
7	EOY19427.1	Cc-nbs-Irr resistance protein, putative [<i>Theobroma cacao</i>]	309,414	5.19	276	−2,2	DR
8	EOX91250.1	Photosystem II subunit O-2 [<i>Theobroma cacao</i>]	35,364	5.85	334	4	P
24	EOY02403.1	Carbonic anhydrase 1 isoform 2 [<i>Theobroma cacao</i>]	35,284	8.35	643	2	OP
38	XP_017985371	60 kDa jasmonate-induced -like [<i>Theobroma cacao</i>]	54,475	4.84	582	1,9	DR
42	EOX97285.1	Malate dehydrogenase isoform 1 [<i>Theobroma cacao</i>]	41,725	9.0	346	5,6	OR
43	EOX97285.1	Malate dehydrogenase isoform 1 [<i>Theobroma cacao</i>]	36,001	5.70	313	2,3	OR
46	XP_007026083.1	ATP synthase gamma chain, chloroplastic [<i>Theobroma cacao</i>]	41,685	5.57	349	6,5	ATP
48	XP_007032095.1	Glyceraldehyde-3-phosphate dehydrogenase A, chloroplastic [<i>Theobroma cacao</i>]	43,255	8.15	887	2,3	C
53	XP_007032095.1	Glyceraldehyde-3-phosphate dehydrogenase A, chloroplastic [<i>Theobroma cacao</i>]	43,255	8.15	582	2,6	C
63	XP_007026120.1	Aminomethyltransferase, mitochondrial [<i>Theobroma cacao</i>]	44,708	8.86	80	1,86	NC
64	XP_007026120.1	Aminomethyltransferase, mitochondrial [<i>Theobroma cacao</i>]	44,708	8.86	80	1,6	NC
67	AET06145.1	Pyridoxal phosphate-dependent aminotransferase (PLP) [<i>Papaver somniferum</i>]	53,606	6.16	73	−1,5	OP
71	Q05991.1	RuBisCO large chain; Short=RuBisCO large subunit [<i>Theobroma cacao</i>]	49,908	5.95	555	−2	P
72	AGD79694.1	RuBisCO [<i>Brosimum Guyanense</i>]	51,328	6.0	409	−1,6	P
74	CAA04978.1	RuBisCO, partial (chloroplast) [<i>Neuburgia corynocarpum</i>]	52,163	6.14	883	1,5	P
77	AEE01402.1	ATP synthase beta chain, partial (chloroplast) [<i>Luehea divaricata</i>]	53,020	5.28	707	5,8	ATP
82	ADO64898.2	RuBisCO large subunit (chloroplast) [<i>Theobroma cacao</i>]	53,512	6.04	514	2	P
86	ADO64898.2	RuBisCO large subunit (chloroplast) [<i>Theobroma cacao</i>]	53,512	6.04	673	4,7	P
89	YP_004021302.1	ATP synthase CF1 alpha subunit [<i>Theobroma cacao</i>]	55,336	5.19	941	2	ATP
90	EOY34440.1	RuBisCO large subunit-binding protein subunit alpha isoform 1 [<i>Theobroma cacao</i>]	64,075	5.06	272	1,8	PF
91	YP_004021302.1	ATP synthase CF1 alpha subunit [<i>Theobroma cacao</i>]	55,336	5.19	772	2,2	ATP
96	ACR38891.1	Heat shock protein 70 [<i>Apopellia endiviifolia</i>]	71,530	5.03	198	7,9	PF/DR
97	XP_008787626.1	DNA ligase 6-like [<i>Phoenix dactylifera</i>]	158,222	6.94	54	40	DR
98	XP_007034724.1	Photosystem I reaction center subunit II, chloroplastic [<i>Theobroma cacao</i>]	23,284	9.6	344	∞	P
100	XP_008787626.1	DNA ligase 6-like [<i>Phoenix dactylifera</i>]	158,222	6.94	54	∞	DR
101	EOX91250.1	Photosystem II subunit O-2 [<i>Theobroma cacao</i>]	35,364	5.85	300	∞	P
102	EOX91250.1	Photosystem II subunit O-2 [<i>Theobroma cacao</i>]	35,364	5.85	860	∞	P
104	EOX91250.1	Photosystem II subunit O-2 [<i>Theobroma cacao</i>]	35,364	5.85	297	∞	P
105	EOY11059.1	Pathogenesis-related protein PR-4 [<i>Theobroma cacao</i>]	30,647	4.15	58	∞	DR
107	XP_017978306.1	Ferredoxin–NADP reductase, leaf isozyme, chloroplastic [<i>Theobroma cacao</i>]	46,018	9.02	391	∞	OR/P
108	EOY11059.1	Pathogenesis-related protein PR-4 [<i>Theobroma cacao</i>]	30,647	4.15	641	∞	DR
109	EOY21247.1	Putative 21 kDa Trypsin Inhibitor [<i>Theobroma bicolor</i>]	24,264	5.71	62	∞	PM
112	XP_007032095.1	Glyceraldehyde-3-phosphate dehydrogenase A, chloroplastic [<i>Theobroma cacao</i>]	43,279	8.43	345	∞	C
113	AIZ00507.1	Glyceraldehyde 3-phosphate dehydrogenase, partial [<i>Salvia officinalis</i>]	21,578	6.67	124	∞	C
116	ADB81493.1	Glyceraldehyde-3-phosphate dehydrogenase, partial [<i>Nephroselmis olivacea</i>]	18,682	6.17	82	∞	C
117	XP_010263896.1	PREDICTED: fructose-bisphosphate aldolase 1, chloroplastic [<i>Nelumbo nucifera</i>]	42,906	8.18	474	∞	C/NC
118	XP_010496369.1	Formin-binding 4-like isoform X2 [<i>Camelina sativa</i>]	12,286	4.85	59	∞	OP
121	XP_007026083.1	ATP synthase gamma chain, chloroplastic [<i>Theobroma cacao</i>]	41,685	5.57	492	∞	ATP
122	XP_007040771.1	Phosphoribulokinase, chloroplastic [<i>Theobroma cacao</i>]	45,827	6.22	352	∞	C/NC
123	P27774.1	Phosphoribulokinase, chloroplastic [<i>Theobroma cacao</i>]	44,486	6.03	86	∞	C/NC
130	XP_008787626.1	DNA ligase 6-like [<i>Phoenix dactylifera</i>]	158,222	6.94	54	∞	DR
132	XP_017980600.1	Phosphoglycerate kinase, chloroplastic [<i>Theobroma cacao</i>]	51,447	8.49	1,075	∞	C/NC
133	XP_002513353.1	Phosphoglycerate kinase, chloroplastic [<i>Ricinus communis</i>]	50,114	8.74	150	∞	C/NC
134	XP_017973236.1	Elongation factor Tu, chloroplastic [<i>Theobroma cacao</i>]	52,371	6.45	230	∞	PM
136	XP_008787626.1	DNA ligase 6-like [<i>Phoenix dactylifera</i>]	158,222	6.94	54	0	DR
137	YP_004021323.1	ATP synthase CF1 beta subunit [<i>Theobroma cacao</i>]	53,693	5.29	1,903	∞	ATP
138	YP_004021323.1	ATP synthase CF1 beta subunit [<i>Theobroma cacao</i>]	53,693	5.29	1,448	∞	ATP
139	YP_004021323.1	ATP synthase CF1 beta subunit [<i>Theobroma cacao</i>]	53,693	5.29	1,921	∞	ATP
140	AIB03257.1	RuBisCO [<i>Fridericia chica</i>]	19,514	6.18	54	∞	P

(Continued)

TABLE 2 | Continued

N° Spot ^a	N° Acesso	Nome da proteína e organismo referência	MM ^b	pI ^c	Score ^d	Fold ^e	Proc. Biol. ^f
141	YP_004021323.1	ATP synthase CF1 beta subunit [<i>Theobroma cacao</i>]	53,693	4.95	1,907	∞	ATP
142	AKR17225.1	ATP synthase beta subunit, partial (chloroplast) [<i>Dioscorea maciba</i>]	31,562	4.54	61	∞	ATP
143	YP_004021302.1	ATP synthase CF1 alpha subunit [<i>Theobroma cacao</i>]	55,336	5.19	959	∞	ATP
144	AKF00085.1	ATP synthase CF1 alpha subunit (chloroplast) [<i>Orania palindan</i>]	56,213	5.41	234	∞	ATP
146	EOX96247.1	Transketolase [<i>Theobroma cacao</i>]	81,006	6.34	397	∞	OP
147	EOX96247.1	Transketolase [<i>Theobroma cacao</i>]	24,263	5.94	501	∞	OP
148	EOX96247.1	Transketolase [<i>Theobroma cacao</i>]	81,006	6.34	558	∞	OP
150	EOX96247.1	Transketolase [<i>Theobroma cacao</i>]	81,006	6.34	529	∞	OP
152	AAV41233.1	Putative 21 kDa Trypsin Inhibitor [<i>Theobroma bicolor</i>]	24,263	5.94	135	∞	PM
159	KVI02111.1	Aldolase-type TIM barrel [<i>Cynara cardunculus</i> var. <i>scolymus</i>]	35,707	7.78	56	∞	OR
160	KVI02111.1	Aldolase-type TIM barrel [<i>Cynara cardunculus</i> var. <i>scolymus</i>]	35,707	7.78	56	∞	OR
161	KVI02111.1	Aldolase-type TIM barrel [<i>Cynara cardunculus</i> var. <i>scolymus</i>]	35,707	7.78	56	∞	OR
162	EOY13706.1	Aldolase-type TIM barrel family protein isoform 1 [<i>Theobroma cacao</i>]	40,802	9.34	481	∞	OR
163	AAV41233.1	Putative 21 kDa Trypsin Inhibitor [<i>Theobroma bicolor</i>]	24,263	5.94	30	∞	PM
166	CAB00006.1	RuBisCO [<i>Dovyalis rhamnoides</i>]	5,218	6.18	64	∞	P
167	CUR00062.1	AtpA (chloroplast) [<i>Acacia acuaría</i>]	55,478	5.04	245	∞	ATP
168	EOY32236.1	TCP-1/cpn60 chaperonin family protein [<i>Theobroma cacao</i>]	64,513	5.62	454	∞	PF/DR
170	CAA72612.1	RuBisCO (chloroplast) [<i>Spigelia anthelmia</i>]	53,314	6.14	314	∞	P
172	CUR00003.1	rbcl-RubisCO (chloroplast) [<i>Acacia acanthoclada</i> subsp. <i>glaucescens</i>]	53,109	6.17	62	∞	P
174	EOY19427.1	Cc-nbs-lrr resistance protein, putative [<i>Theobroma cacao</i>]	309,414	5.19	71	∞	DR
175	AAV41233.1	Putative 21 kDa Trypsin Inhibitor [<i>Theobroma bicolor</i>]	24,263	5.94	812	∞	PM
177	AAV41233.1	Putative 21 kDa Trypsin Inhibitor [<i>Theobroma bicolor</i>]	24,263	5.94	501	∞	PM
178	AAV41233.1	Putative 21 kDa Trypsin Inhibitor [<i>Theobroma bicolor</i>]	24,264	5.71	211	∞	PM
180	XP_007034724.1	Photosystem I reaction center subunit II, chloroplastic [<i>Theobroma cacao</i>]	23,284	9.6	313	∞	P
183	EOX91250.1	Photosystem II subunit O-2 [<i>Theobroma cacao</i>]	35,364	5.85	1,027	0	P
184	KVH98530.1	Malate dehydrogenase isoform 1 [<i>Theobroma cacao</i>]	43,464	7.64	138	∞	OR
185	AAV41233.1	Putative 21 kDa Trypsin Inhibitor [<i>Theobroma bicolor</i>]	24,264	5.71	188	0	PM
192	XP_017985371	60 kDa jasmonate-induced -like [<i>Theobroma cacao</i>]	54,475	5.84	195	0	DR
195	XP_008787626.1	DNA ligase 6-like [<i>Phoenix dactylifera</i>]	158,222	6.94	54	0	DR
196	OIW04199.1	PREDICTED: oxygen-enhancing protein 2-1, chloroplastic [<i>Lupinus angustifolius</i>]	27,943	8.39	56	0	P
198	EOY19508.1	23 kDa jasmonate-induced protein-like [<i>Durio zibethinus</i>]	25,321	5.6	382	0	DR
200	XP_007025148.1	Chlorophyll a-b binding protein of LHCII type 1 [<i>Theobroma cacao</i>]	28,219	5.13	372	0	P/DR
203	XP_007025148.1	Chlorophyll a-b binding protein of LHCII type 1 [<i>Theobroma cacao</i>]	28,219	5.13	304	0	P/DR
209	EOX91250.1	Photosystem II subunit O-2 [<i>Theobroma cacao</i>]	158,222	6.94	54	0	P
213	EOX91250.1	Photosystem II subunit O-2 [<i>Theobroma cacao</i>]	35,364	5.85	896	0	P
229	XP_007032095.1	Glyceraldehyde 3-phosphate dehydrogenase A, cloroplasto [<i>Theobroma cacao</i>]	35,364	5.85	699	0	C
231	XP_007032095.1	Glyceraldehyde 3-phosphate dehydrogenase A, cloroplasto [<i>Theobroma cacao</i>]	43,255	8.15	533	0	C
233	EOY02669.1	Glyceraldehyde 3-phosphate dehydrogenase C2 isoforma 1 [<i>Theobroma cacao</i>]	43,255	8.15	753	0	C
235	AGB05600.1	Fructose-bisfosfato-aldolase 3 [<i>Camellia oleifera</i>]	43,094	8.44	287	0	C/NC
241	XP_007040771.1	Phosphoribulokinase,cloroplasmático [<i>Theobroma cacao</i>]	45,827	6.22	403	0	C/NC
242	XP_007040771.1	Phosphoribulokinase, chloroplastic [<i>Theobroma cacao</i>]	45,827	6.22	506	0	C/NC
244	XP_008787626.1	DNA ligase 6-like [<i>Phoenix dactylifera</i>]	158,222	6.94	53	0	DR
248	XP_008787626.1	DNA ligase 6-like [<i>Phoenix dactylifera</i>]	158,222	6.94	54	0	DR
249	XP_007041810.1	Glycerate dehydrogenase [<i>Theobroma cacao</i>]	42,522	7.60	345	0	OR
251	EOY07449.1	RuBisCO 1 isoform 1 [<i>Theobroma cacao</i>]	62,893	8.77	204	0	P
253	XP_007009267.1	RuBisCO activase 2 isoform X2 [<i>Theobroma cacao</i>]	48,566	5.56	357	0	DR
254	XP_007009267.1	RuBisCO activase 2, isoform X2 [<i>Theobroma cacao</i>]	48,566	5.56	340	0	DR
257	EOY15330.1	Glyceraldehyde-3-phosphate dehydrogenase B subunit [<i>Theobroma cacao</i>]	48,483	6.76	256	0	C
259	Q7X999.1	RuBisCO activase 2, chloroplastic [<i>Theobroma cacao</i>]	48,251	6.78	56	0	DR
261	AAF04851.1	Putative alcohol dehydrogenase [<i>Hibiscus syriacus</i>]	42,527	6.56	68	0	OR
262	ABK00052.1	Glyceraldehyde-3-phosphate dehydrogenase, Chloroplast [<i>Marchantia polymorpha</i>]	38,618	6.60	53	0	C

(Continued)

TABLE 2 | Continued

N° Spot ^a	N° Acesso	Nome da proteína e organismo referência	MM ^b	pI ^c	Score ^d	Fold ^e	Proc. Biol. ^f
272	XP_008787626.1	DNA ligase 6-like [<i>Phoenix dactylifera</i>]	158,222	6.94	54	0	DR
287	CAC16593.1	RuBisCO [<i>Oxycceros sp.</i>]	52,659	6.22	460	0	P
289	EOY19427.1	Cc-nbs-Irr resistance protein, putative [<i>Theobroma cacao</i>]	309,414	5.19	727	0	DR
290	YP_913172.1	ATP synthase alpha subunit [<i>Gossypium barbadense</i>]	55,501	5.19	676	0	ATP
298	EOX96247.1	Transketolase [<i>Theobroma cacao</i>]	81,006	6.34	613	0	OP
299	EOX96247.1	Transketolase [<i>Theobroma cacao</i>]	81,006	6.34	285	0	OP
301	EOX96247.1	Transketolase [<i>Theobroma cacao</i>]	81,006	6.34	575	0	OP
303	EOX96247.1	Transketolase [<i>Theobroma cacao</i>]	81,006	6.34	445	0	OP
307	EOY32513.1	Lipoxygenase isoform 1 [<i>Theobroma cacao</i>]	103,618	5.74	509	0	OR
308	AAV41233.1	Putative 21 kDa Trypsin Inhibitor [<i>Theobroma bicolor</i>]	24,263	5.94	280	0	PM
310	OAP02478.1	HSP93-III [<i>Arabidopsis thaliana</i>]	106,001	6.13	66	0	PM
313	AAV41233.1	Putative 21 kDa Trypsin Inhibitor [<i>Theobroma bicolor</i>]	24,263	5.94	785	0	PM
319	XP_018806973.1	Armadillo repeat-containing kinesin-like protein 2 [<i>Juglans regia</i>]	100,848	6.16	54	0	OP
321	KNA04085.1	Glycine dehydrogenase (decarboxylating) mitochondrial [<i>Spinacia oleracea</i>]	114,612	6.68	54	0	OR
324	XP_008787626.1	DNA ligase 6-like [<i>Phoenix dactylifera</i>]	158,222	6.9	54	0	DR
325	EOY02403.1	Carbonic anhydrase 1 isoform 2 [<i>Theobroma cacao</i>]	35,284	8.35	127	0	OP
328	EOY21251.1	Putative 21 kDa Trypsin Inhibitor [<i>Theobroma bicolor</i>]	24,263	5.94	350	0	PM
329	XP_007034724.1	Photosystem I reaction center subunit II, chloroplastic [<i>Theobroma cacao</i>]	23,284	9.96	383	0	P

^aSpot number assigned in the analysis of gels using ImageMaster 2D Platinum 7.0 software, as indicated in Figure 1B.

^bTheoretical molecular weight in Daltons assigned by MASCOT.

^cTheoretical Isoelectric Point assigned by MASCOT.

^dScore assigned by MASCOT, being the sum of the highest score of ions for each distinct sequence.

^eFold corresponds to the alteration in expression between inoculated and control treatments, calculated using ImageMaster 2D Platinum 7.0 software: (0) identified exclusively in the control treatment, (∞) identified exclusively in the inoculated treatment, (+) super accumulated in the inoculated treatment, (-) super accumulated in the control treatment.

^fBiological process to which the protein belongs according to the Blast2GO tool and the Uniprot database: ATP, ATP metabolism; Ph, photosynthesis; DR, defense/response to stress/stimulus; PF, protein folding; PM, protein metabolism; OR, oxide-reduction process; C, carbohydrate metabolism; NC, nitrogen compound metabolism; OP, other processes; Um, not noted.

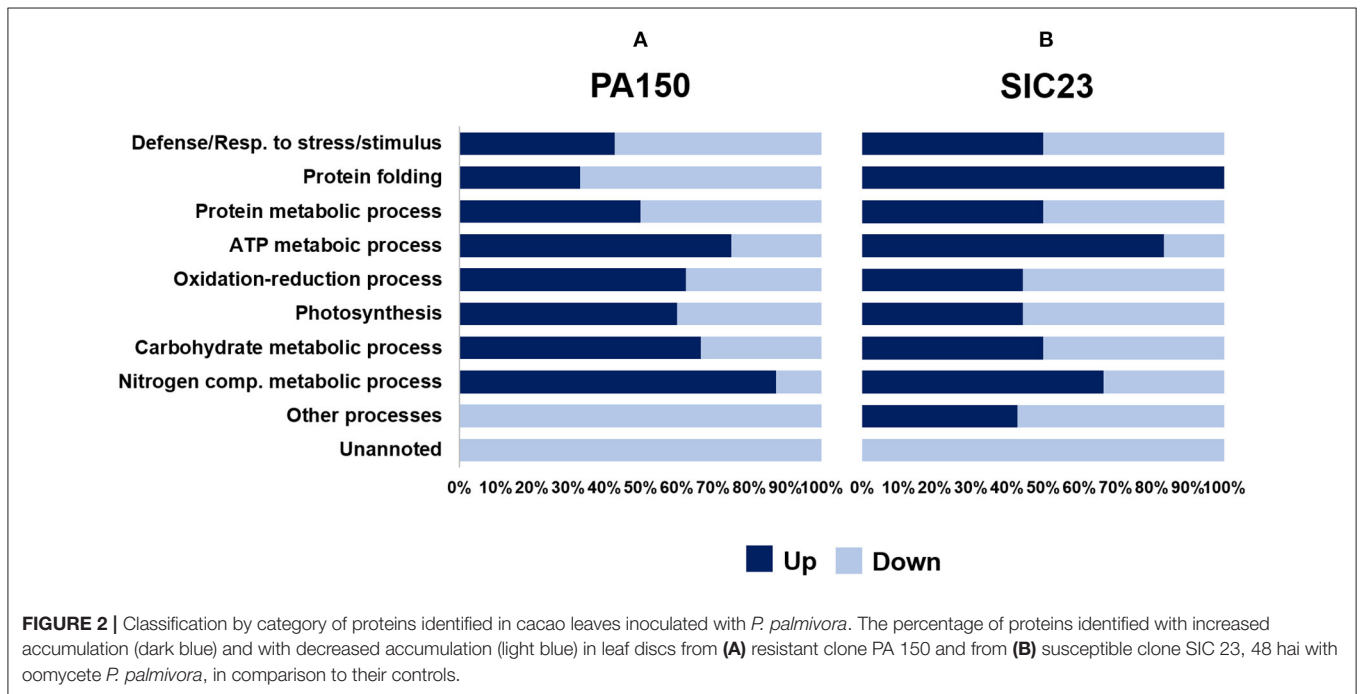


FIGURE 2 | Classification by category of proteins identified in cacao leaves inoculated with *P. palmivora*. The percentage of proteins identified with increased accumulation (dark blue) and with decreased accumulation (light blue) in leaf discs from (A) resistant clone PA 150 and from (B) susceptible clone SIC 23, 48 hai with oomycete *P. palmivora*, in comparison to their controls.

TPI and GAPC Proteins Could Help in the Control of Cytotoxic Metabolites and Protect Against Redox Imbalance in the Resistant Clone

The metabolism of carbohydrates positively regulates the expression of genes related to defense (Rojas et al., 2014). In this regard, it was observed that the triosephosphate isomerase enzyme (TPI) (Table 1; spot 181) had increased accumulation in the PA 150 clone after inoculation, which is an indication of glycolytic pathway increase (Valcu et al., 2009). In addition, TPI assists in the control of methylglyoxal levels, a cytotoxic metabolite and glycolysis by-product, which is accumulated in plants under stress and which participates as a molecular signaler (Kaur et al., 2015).

In turn, the glyceraldehyde-3-phosphate-dehydrogenase (GAPDH) protein, in its cytosolic form (GAPC), intermediates in both energy metabolism and signal transference for long-term adjustment and protection against redox imbalance (Schneider et al., 2018). In the pathosystem *T. cacao*–*M. perniciosa*, two GAPC isoforms were identified with increased accumulation in the resistant clone at 72 hai (dos Santos et al., 2020). Interestingly, a GAPC had differentiated accumulation between the clones since it was super accumulated in the PA 150 clone (spot 193) and had reduced accumulation in the SIC 23 clone (spot 233), which may influence the resistance of *T. cacao* to *P. palmivora*. This is also represented in the interaction network of the resistant clone (Figure 3A; Supplementary Table 7), in which the cluster where the GAPC isoforms meet had assigned processes for glucose metabolism and cellular redox homeostasis.

Photosynthesis and Metabolism of Sugars Are the Most Affected Processes During *P. palmivora* Infection

The fact that the clusters with a greater number of proteins were those related to photosynthesis and metabolism of sugar (Supplementary Tables 5, 6) suggests that these biological functions were the most affected during *P. palmivora* infection. Network analysis demonstrates that the proteins homologous to those identified in SIC 23 with reduced accumulation have greater influence on the clusters corresponding to processes of photosynthesis and metabolism of sugars in comparison to the proteins homologous to those identified with increased accumulation, based on node degree value. The opposite occurs in the PA 150 clone, where the proteins homologous to those identified with increased accumulation have a higher node degree value. This may translate into an increase in the resistant clone and a decrease in the susceptible clone for these biological processes.

A Phosphoribulokinase Could Be Involved in Resistance to *P. palmivora*

A phosphoribulokinase (PRK) was found to be differentially expressed (Tables 1, 2). In the inoculated PA 150 clone, all of the spots corresponding to PRK (spots 76, 187, and 196) had increased accumulation. However, in the SIC 23 clone, the PRK protein varied in accumulation between the different

spots, with two of them (spots 122 and 123) showing increased accumulation and the other two (spots 241 and 242) showing decreased accumulation after inoculation. This protein was identified as repressed in susceptible black pepper inoculated with *Phytophthora capsici* (Mahadevan et al., 2016) and is involved in the defense response to bacteria in Arabidopsis (Jones et al., 2006). Therefore, this difference in the accumulation pattern may be involved in resistance in the PA 150 clone. Furthermore, the PRK is regulated by thioredoxin (Feierabend, 2005), which was identified in two spots in the inoculated PA 150 clone (Table 1); one with increased accumulation (spot 18) and the other with reduced accumulation (spot 293).

Lipoxygenase Involved in Jasmonic Acid Production and Substances Antimicrobials Production in Resistant Clone

Lipoxygenase (LOX) was identified as up-accumulated in the PA 150 clone and down-accumulated in the SIC 23 clone (Table 1, spot 224; Table 2, spot 307). In tobacco plants inoculated with *Phytophthora parasitica nicotianae*, it was observed that LOX gene transcripts increased and their activity was increased in the initial stages of infection in resistant plants (Veronesi et al., 1996). The LOX pathway results in the production of taumatins, JA, oxylipins, and volatile aldehydes that play an important role in wound healing, synthesis of antimicrobial substances, and membrane damage during the hypersensitive response (HR) (Thakur and Udayashankar, 2019). Jasmonic acid enhances superoxide production and activates genes encoding proteins involved in defense responses (Vasyukova and Ozeretskovskaya, 2009; Karpets et al., 2014), increases resistance to *Phytophthora infestans* in tomatoes and potatoes (Cohen et al., 1993) and the defense measured by this hormone is crucial to the resistance of peppers to *P. capsici* (Ueeda et al., 2005).

An Enone Oxidoreductase Involved in Biosynthesis of Volatile Compounds Is Up-Accumulated in the Resistant Clone

After inoculation, 2-methylene-furan-3-one reductase-like (enone oxidoreductase) was found to increase accumulation in the resistant genotype. This protein is induced by ripening and inhibited by auxin in strawberries (Schiefner et al., 2013). It was also found only in the *Prunus persica* clone resistant to the fungus *Taphrina deformans* (Goldy et al., 2017). Furthermore, the protein is involved in the biosynthesis of furaneol, which is a volatile compound (Raab et al., 2006) that may be involved in defense signaling (Peinado-Guevara et al., 2017). The homolog of this protein in the network is AOR, a NADPH dependent oxidoreductase, that aids in detoxifying stromal reactive carbonyls produced under oxidative stress (Yamauchi et al., 2011, 2012).

A Probable CC-NBS-LRR Protein May Be Key in Cacao Resistance Against *P. palmivora*

A probable CC-NBS-LRR protein was identified in both clones, albeit with different accumulation patterns. In the SIC 23 clone,

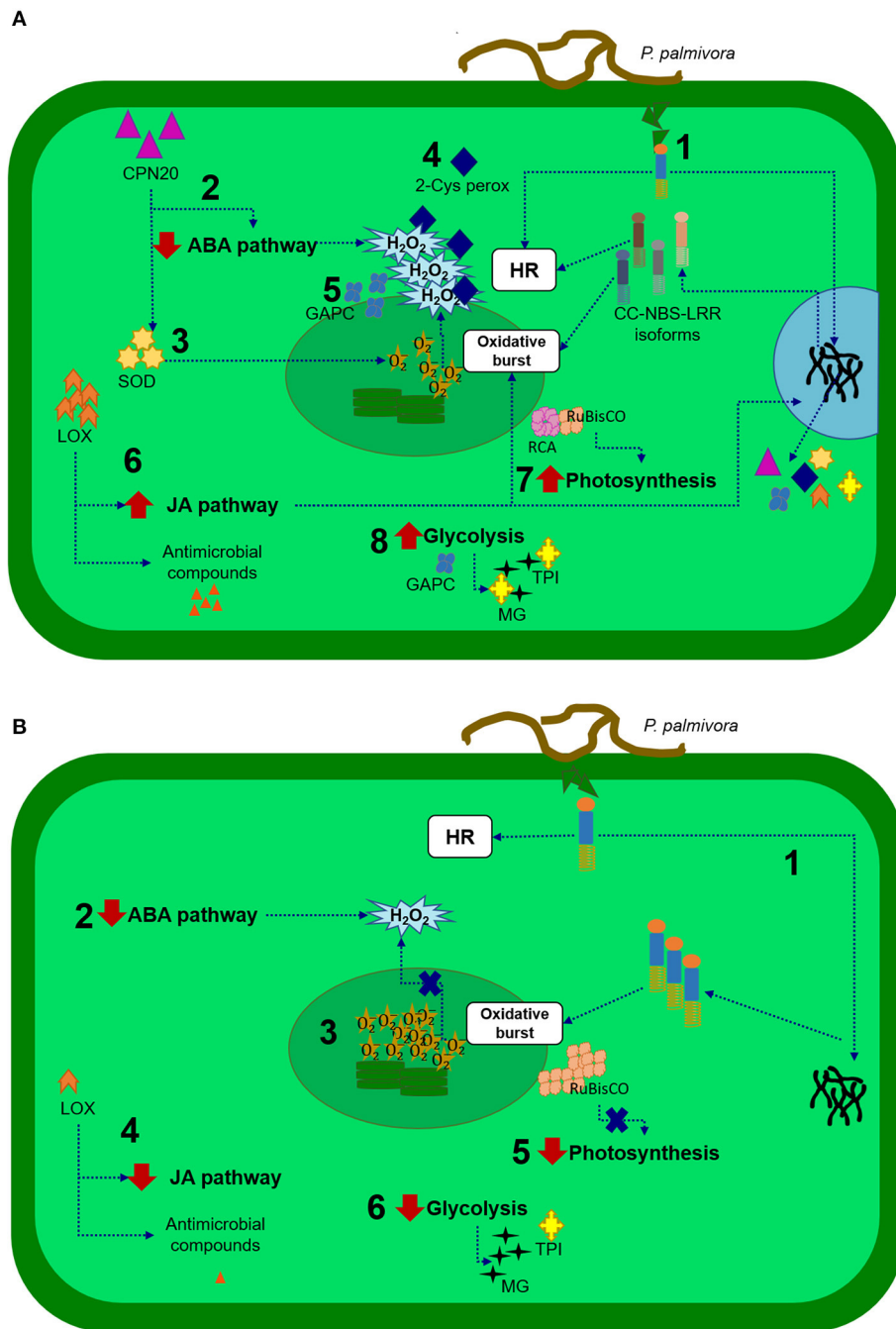


FIGURE 4 | Representative scheme of the defense responses of the cacao tree to *P. palmivora*. In the resistant clone **(A)**: (1) A CC-NBS-LRR protein recognizes products derived from the pathogen, initiating a response that includes hypersensitive response (HR) and signaling for expression of isoforms and other proteins that help in defense responses; (2) CPN20 protein negatively regulates the signaling of ABA, promoting H₂O₂ accumulation; (3) CPN20 also activates superoxide dismutase (SOD) enzymes that dismutate superoxide in H₂O₂ and O₂; (4) 2-cys peroxidoredoxin regulates H₂O₂ concentration; (5) A cytosolic glyceraldehyde-3-phosphate-dehydrogenase (GAPC) protect against redox imbalance; (6) A lipoxygenase (LOX) protein activates jasmonic acid (JA) production, which enhances superoxide production and activates genes encoding proteins involved in defense responses; (7) RuBisCO activase (RCA) is increased, assisting in the activity of RuBisCO increasing photosynthesis and (8) Active glycolysis, where the triosephosphate isomerase (TPI) enzyme assists in the control of methylglyoxal levels (MG), a cytotoxic by-product of glycolysis. In the susceptible clone **(B)**: (1) A CC-NBS-LRR protein recognizes products derived from the pathogen. This isoform could initiate responses like HR, but there would be no expression of other isoforms; (2) ABA pathway reduced allows the accumulation of H₂O₂; (3) In CPN20, 2-Cys peroxidoredoxin or GAPC accumulation could lead to imbalance redox; (4) Decrease in LOX accumulation causes a decrease in the production of jasmonic acid and antimicrobial compounds; (5) RuBisCO not activated can affect photosynthesis; (6) Glycolysis pathway is reduced, and production of TPI could be insufficient to protect against cytotoxic compounds.

three spots (Table 2; spots 7, 174, and 289) were identified corresponding to this protein, whereby only one of them had increased accumulation. In the PA 150 clone, seven spots were identified corresponding to the same protein (Table 1); five had increased accumulation (spots 159, 178, 211, 212, and 215) and two (spots 251 and 41) reduced accumulation.

The CC-NBS-LRR proteins are codified by one of the genes identified as genes of plant resistance (R) to diseases. Their structure contains an N-terminal coiled-coil (CC) domain, a nucleotide binding site (NBS) domain, and a C-terminal leucine-rich repeat (LRR) domain. The CC-NBS-LRR proteins recognize products derived from specific pathogens and initiate a resistance response that generally includes a type of cell death known as hypersensitivity response (HR) (Moffett et al., 2002). It has already been observed that the expression of this protein confers resistance to *P. infestans* on currant tomatoes (Zhang et al., 2014) and positive regulation was discovered for various NBS-LRR genes that suppress *P. infestans* infection in *Solanum pinnatisectum* (Gu et al., 2020). The cacao genome contains several copies corresponding to the genes that encodes CC-NBS-LRR isoforms (<https://cocoa-genome-hub.southgreen.fr>). Therefore, the accumulation of the different spots correspondent to this protein in PA 150 suggests that this clone can express more isoforms of this protein than the susceptible clone, giving it an advantage in its defense mechanism against *P. palmivora*.

CONCLUSIONS

Leaves from PA 150 (resistant) and SIC 23 (susceptible) clones of *T. cacao* inoculated with *P. palmivora* present differences in the protein profile when compared with their respective controls (mock-inoculated). These differences revealed evidence of the defense mechanisms presented in each clone (Figure 4).

According to the expression pattern of various identified proteins, processes of photosynthesis, and metabolism of sugars increase in the resistant clone and decrease in the susceptible clone and were apparently the most affected processes during *P. palmivora* infection.

RuBisCO Activase is thought to be a protein that plays an important role in regulation and signaling both clones defense responses. The reduction in the quantity of RCA in the SIC 23 clone suggests deficient rubisco activity, and, therefore, energy decline in the cell. Thus, increased accumulation of rubisco and ATP synthase is being attempted to compensate for this energy loss.

In the resistant clone, there was evidence of better management of ROS production and regulation and in the control of cytotoxic by-products of glycolysis, and protection against redox imbalances, reduction in the ABA pathway, and, therefore, accumulation of H₂O₂. In addition, the increased

accumulation of the LOX protein suggests production of JA, oxylipins, and volatile aldehydes important in wound healing, synthesis of antimicrobial substances, and membrane damage during the HR. It has already been demonstrated that JA is involved in the resistance of plants to *Phytophthora* species. In turn, an oxidoreductase may contribute to detoxifying compounds produced under oxidative stress, and a probable CC-NBS-LRR protein recognizes products derived from the pathogen, initiating a response that includes a HR.

DATA AVAILABILITY STATEMENT

The datasets presented in this study can be found in online repositories. The names of the repository/repositories and accession number(s) can be found in the article/Supplementary Material.

AUTHOR CONTRIBUTIONS

AR, EL, and RC contributed to the conception and design of the study. AR and IM-O organized the database and performed the statistical analysis. AR wrote the first draft of the manuscript. CP supervised the proteomics analysis. EL and RX supervised the phytopathological experiments and obtained financial support for the project. All authors contributed to manuscript revision, read, and approved the submitted version.

FUNDING

This work was supported by the Conselho Nacional de Ciência e Tecnologia – CNPq, a Brazilian Federal Government agency (grant number 309841/2015-1 and 308959/2019-1); and the Coordenação de Aperfeiçoamento de Pessoal de Nível Superior – CAPES, Bahian State Government (Scholarship number 481074/2013-9 e 307915/2012-3 granted to AR).

ACKNOWLEDGMENTS

The authors are grateful to Comissão Executiva do Plano da Lavoura Cacaueira – CEPLAC, for their assistance in preparing *Phytophthora* zoospores for cocoa inoculation, and Universidade Estadual de Santa Cruz – UESC, for providing the facilities in Greenhouse and Center of Biotechnology and Genetics CBG.

SUPPLEMENTARY MATERIAL

The Supplementary Material for this article can be found online at: <https://www.frontiersin.org/articles/10.3389/fagro.2022.836360/full#supplementary-material>

REFERENCES

Adeniyi, D. (2019). “Diversity of cacao pathogens and impact on yield and global production,” in *Theobroma Cacao - Deploying Science for Sustainability of Global Cocoa Economy*, ed P. Aikpokpodion (London: IntechOpen). doi: 10.5772/intechopen.81993 Available online at: <https://www.intechopen.com/chapters/65131>

Ali, S. S., Shao, J., Lary, D. J., Strem, M. D., Meinhardt, L. W., and Bailey, B. A. (2017). *Phytophthora megakarya* and *P. palmivora*, causal agents of black pod rot, induce similar plant defense responses late during infection of susceptible cacao pods. *Front. Plant Sci.* 8, 169. doi: 10.3389/fpls.2017.00169

Almeida, D. S. M., Gramacho, K. P., Cardoso, T. H. S., Micheli, F., Alvim, F. C., and Pirovani, C. P. (2017). Cacao phylloplane: the first battlefield

- against *Moniliophthora perniciosa*, which causes witches' broom disease. *Phytopathology* 107, 864–871. doi: 10.1094/PHYTO-06-16-0226-R
- Argout, X., Fouet, O., Wincker, P., Gramacho, K., Legavre, T., Sabau, X., et al. (2008). Towards the understanding of the cocoa transcriptome: production and analysis of an exhaustive dataset of ESTs of *Theobroma cacao* L. generated from various tissues and under various conditions. *BMC Genomics* 9, 512. doi: 10.1186/1471-2164-9-512
- Asada, K. (2006). Production and scavenging of reactive oxygen species in chloroplasts and their functions. *Plant Physiol.* 141, 391–396. doi: 10.1104/pp.106.082040
- Asselbergh, B., De Vleeschauwer, D., and Höfte, M. (2008). Global switches and fine-tuning—ABA modulates plant pathogen defense. *Mol. Plant Microbe Interact.* 21, 709–719. doi: 10.1094/MPMI-21-6-0709
- Awad, J., Stotz, H. U., Fekete, A., Krischke, M., Engert, C., Havaux, M., et al. (2015). 2-Cysteine peroxidoredoxins and thylakoid ascorbate peroxidase create a water-water cycle that is essential to protect the photosynthetic apparatus under high light stress conditions. *Plant Physiol.* 167, 1592–1603. doi: 10.1104/pp.114.255356
- Bailey, B. A., Ali, S. S., Akrofi, A. Y., and Meinhardt, L. W. (2016). “*Phytophthora megakarya*, a causal agent of black pod rot in Africa,” in eds B. A. Bailey and L. W. Meinhardt, *Cacao Diseases* (Cham: Springer International Publishing), 267–303. doi: 10.1007/978-3-319-24789-2_8
- Barreto, M. A., Santos, J. C. S., Corrêa, R. X., Luz, E. D. M. N., Marelli, J., and Souza, A. P. (2015). Detection of genetic resistance to cocoa black pod disease caused by three *Phytophthora* species. *Euphytica* 206, 677–687. doi: 10.1007/s10681-015-1490-4
- Bowers, J. H., Bailey, B. A., Hebbbar, P. K., Sanogo, S., and Lumsden, R. D. (2001). The impact of plant diseases on world chocolate production. *Plant Health Prog.* 2, 12. doi: 10.1094/PHP-2001-0709-01-RV
- Carmo-Silva, A. E., and Salvucci, M. E. (2011). The activity of Rubisco's molecular chaperone, rubisco activase, in leaf extracts. *Photosynth Res.* 108, 143–155. doi: 10.1007/s11120-011-9667-8
- Cohen, Y., Gisi, U., and Niderman, T. (1993). Local and systemic protection against *Phytophthora infestans* induced in potato and tomato plants by jasmonic acid and jasmonic methyl ester. *Phytopathology* 83, 1054–1062. doi: 10.1094/Phyto-83-1054
- Dantas Neto, A., Corrêa, R. X., Monteiro, W. R., Luz, E. D. M. N., Gramacho, K. P., and Lopes, U. V. (2005) Caracterização de uma população de cacauzeiro para mapeamento de genes de resistência à vassoura-de-bruxa e podridão parda. *Fitopatol. Bras.* 30, 380–386. doi: 10.1590/S0100-41582005000400007
- dos Santos, E. C., Pirovani, C. P., Correa, S. C., Micheli, F., and Gramacho, K. P. (2020). The pathogen *Moniliophthora perniciosa* promotes differential proteomic modulation of cacao genotypes with contrasting resistance to witches' broom disease. *BMC Plant Biol.* 20, 1. doi: 10.1186/s12870-019-2170-7
- Feierabend, J. (2005). “Catalases in plants: molecular and functional properties and role in stress defence,” in *Antioxidants and Reactive Oxygen Species in Plants*, ed N. Smirnoff (Oxford: Blackwell Publishing Ltd.), 101–130.
- Geddes, J., Eudes, F., Laroche, A., and Selinger, L. B. (2008). Differential expression of proteins in response to the interaction between the pathogen *Fusarium graminearum* and its host, *Hordeum vulgare*. *Proteomics* 8, 545–554. doi: 10.1002/pmic.200700115
- Goldy, C., Svetaz, L. A., Bustamante, C. A., Allegrini, M., Valentini, G. H., Drincovich, M. F., et al. (2017). Comparative proteomic and metabolomic studies between *Prunus persica* genotypes resistant and susceptible to *Taphrina deformans* suggest a molecular basis of resistance. *Plant Physiol. Biochem.* 118, 245–255. doi: 10.1016/j.plaphy.2017.06.022
- Gu, B., Cao, X., Zhou, X., Chen, Z., Wang, Q., Liu, W., et al. (2020). The histological, effectoromic, and transcriptomic analyses of *Solanum pinnatisectum* reveal an upregulation of multiple NBS-LRR genes suppressing *Phytophthora infestans* infection. *Int. J. Mol. Sci.* 21:9.3211. doi: 10.3390/ijms21093211
- Jansson, S. (1994). The light-harvesting chlorophyll ab-binding proteins. *Biochim Biophys. Acta Bioenerg.* 1184, 1–19. doi: 10.1016/0005-2728(94)90148-1
- Jones, A. M. E., Thomas, V., Bennett, M. H., Mansfield, J., and Grant, M. (2006). Modifications to the Arabidopsis defense proteome occur prior to significant transcriptional change in response to inoculation with *Pseudomonas syringae*. *Plant Physiol.* 142, 1603–1620. doi: 10.1104/pp.106.0.86231
- Karpets, Y. V., Kolupaev, Y. E., Lugovaya, A. A., and Oboznyi, A. I. (2014). Effect of jasmonic acid on the pro-/antioxidant system of wheat coleoptiles as related to hyperthermia tolerance. *Russ. J. Plant Physiol.* 61, 339–346. doi: 10.1134/S102144371402006X
- Kaur, C., Sharma, S., Singla-Pareek, S. L., and Sopory, S. K. (2015). “Methylglyoxal, triose phosphate isomerase, and glyoxalase pathway: implications in abiotic stress and signaling in plants,” in *Elucidation of Abiotic Stress Signaling in Plants* (New York, NY: Springer), 347–366. doi: 10.1007/978-1-4939-2211-6_13
- Kuo, W. Y., Huang, C. H., and Jinn, T. L. (2013b). Chaperonin 20 might be an iron chaperone for superoxide dismutase in activating iron superoxide dismutase (FeSOD). *Plant Signal. Behav.* 8, 2. doi: 10.4161/psb.23074
- Kuo, W. Y., Huang, C. H., Liu, A. C., Cheng, C. P., Li, S. H., Chang, W. C., et al. (2013a). CHAPERONIN 20 mediates iron superoxide dismutase (FeSOD) activity independent of its co-chaperonin role in *Arabidopsis chloroplasts*. *New Phytol.* 197, 99–110. doi: 10.1111/j.1469-8137.2012.04369.x
- Liu, R., Xu, Y.-H., Jiang, S.-C., Lu, K., Lu, Y.-F., Feng, X.-J., et al. (2013). Light-harvesting chlorophyll a/b-binding proteins, positively involved in abscisic acid signalling, require a transcription repressor, WRKY40, to balance their function. *J. Exp. Bot.* 64, 5443–5456. doi: 10.1093/jxb/ert307
- Luz, E. D. M. N., Silva, S. D. V. M., Bezerra, J. L., Souza, J. T., de, and Santos, A. F., dos. (2008). *Glossário Ilustrado de Phytophthora: Técnicas Especiais para o Estudo de Oomicetos*. Itabuna, BA: Fapesb.
- Macagnan, D., Romeiro, R. D. S., de Souza, J. T., and Pomella, A. W. V. (2006). Isolation of actinomycetes and endospore-forming bacteria from the cacao pod surface and their antagonistic activity against the witches' broom and black pod pathogens. *Phytoparasitica* 34, 122–132. doi: 10.1007/BF02981312
- Mahadevan, C., Krishnan, A., Saraswathy, G. G., Surendran, A., Jaleel, A., and Sakuntala, M. (2016). Transcriptome- assisted label-free quantitative proteomics analysis reveals novel insights into *Piper nigrum*—*Phytophthora capsici* phytopathosystem. *Front. Plant Sci.* 7, 785. doi: 10.3389/fpls.2016.00785
- Marelli, J.-P., Guest, D. I., Bailey, B. A., Evans, H. C., Brown, J. K., Junaid, M., et al. (2019). Chocolate under threat from old and new cacao diseases. *Phytopathology* 109, 1331–1343. doi: 10.1094/phyto-12-18-0477-rvw
- Mares, J. H., Gramacho, K. P., Santana, J. O., Oliveira de Souza, A., Alvim, F. C., and Pirovani, C. P. (2020). Hydrosoluble phyloplane components of *Theobroma cacao* modulate the metabolism of *Moniliophthora perniciosa* spores during germination. *Fungal Biol.* 124, 73–81. doi: 10.1016/j.funbio.2019.11.008
- Moffett, P., Farnham, G., Peart, J., and Baulcombe, D. C. (2002). Interaction between domains of a plant NBS-LRR protein in disease resistance-related cell death. *EMBO J.* 21, 4511–4519. doi: 10.1093/emboj/cdf453
- Neuhoff, V., Arold, N., Taube, D., and Ehrhardt, W. (1988). Improved staining of proteins in polyacrylamide gels including isoelectric focusing gels with clear background at nanogram sensitivity using Coomassie Brilliant Blue G-250 and R-250. *Electrophoresis* 9, 255–262. doi: 10.1002/elps.1150090603
- Nyassé, S., Cilas, C., Herail, C., and Blaha, G. (1995). Leaf inoculation as an early screening test for cocoa (*Theobroma cacao* L.) resistance to *Phytophthora* black pod disease. *Crop Prot.* 14, 657–663. doi: 10.1016/0261-2194(95)00054-2
- Oukarroum, A., Bussotti, F., Goltsev, V., and Kalaji, H. M. (2015). Correlation between reactive oxygen species production and photochemistry of photosystems I and II in *Lemna gibba* L. plants under salt stress. *Environ. Exp. Bot.* 109, 80–88. doi: 10.1016/j.envexpbot.2014.08.005
- Peinado-Guevara, L. I., López-Meyer, M., López-Valenzuela, J. A., Maldonado-Mendoza, I. E., Galindo-Flores, H., Campista-León, S., et al. (2017). Comparative proteomic analysis of leaf tissue from tomato plants colonized with *Rhizophagus irregularis*. *Symbiosis* 73, 93–106. doi: 10.1007/s13199-016-0470-3
- Perrine-Walker, F. (2020). *Phytophthora palmivora*-cocoa interaction. *J. Fungi* 6, 167. doi: 10.3390/jof6030167
- Pirovani, C. P., Carvalho, H. A. S., Machado, R. C. R., Gomes, D. S., Alvim, F. C., Pomella, A. W. V., et al. (2008). Protein extraction for proteome analysis from cacao leaves and meristems, organs infected by *Moniliophthora perniciosa*, the causal agent of the witches' broom disease. *Electrophoresis* 29, 2391–2401. doi: 10.1002/elps.200700743
- Portis, A. R., Li, C., Wang, D., and Salvucci, M. E. (2007). Regulation of rubisco activase and its interaction with Rubisco. *J. Exp. Bot.* 59, 1597–1604. doi: 10.1093/jxb/erm240

- Quirino, B. F., Candido, E. S., Campos, P. F., Franco, O. L., and Krüger, R. H. (2010). Proteomic approaches to study plant–pathogen interactions. *Phytochemistry* 71, 351–362. doi: 10.1016/j.phytochem.2009.11.005
- Raab, T., López-Ráez, J. A., Klein, D., Caballero, J. L., Moyano, E., Schwab, W., et al. (2006). FaQR, required for the biosynthesis of the strawberry flavor compound 4-hydroxy-2,5-dimethyl-3(2H)-furanone, encodes an enone oxidoreductase. *Plant Cell* 18, 1023–1037. doi: 10.1105/tpc.105.039784
- Rojas, C. M., Senthil-Kumar, M., Tzin, V., and Mysore, K. S. (2014). Regulation of primary plant metabolism during plant–pathogen interactions and its contribution to plant defense. *Front. Plant Sci.* 5, 17. doi: 10.3389/fpls.2014.00017
- RStudio Team (2019). *RStudio: Integrated Development for R* (1.2.5033). RStudio, Inc. Available online at: <http://www.rstudio.com/> (accessed July 7, 2018).
- Schiefner, A., Sinz, Q., Neumaier, I., Schwab, W., and Skerra, A. (2013). Structural basis for the enzymatic formation of the key strawberry flavor compound 4-hydroxy-2,5-dimethyl-3(2H)-furanone. *J. Biol. Chem.* 288, 16815–16826. doi: 10.1074/jbc.M113.453852
- Schneider, M., Knuesting, J., Birkholz, O., Heinisch, J. J., and Scheibe, R. (2018). Cytosolic GAPDH as a redox-dependent regulator of energy metabolism. *BMC Plant Biol.* 18, 184. doi: 10.1186/s12870-018-1390-6
- Shannon, P. (2003). Cytoscape: a software environment for integrated models of biomolecular interaction networks. *Genome Res.* 13, 2498–2504. doi: 10.1101/gr.1239303
- Shevchenko, A., Tomas, H., Havlis, J., Olsen, J. V., and Mann, M. (2007). In-gel digestion for mass spectrometric characterization of proteins and proteomes. *Nat. Protoc.* 1, 2856–2860. doi: 10.1038/nprot.2006.468
- Silva, F. A. C., Pirovani, C. P., Menezes, S., Pungartnik, C., Santiago, A. S., Costa, M. G. C., et al. (2013). Proteomic response of *Moniliophthora perniciosa* exposed to pathogenesis-related protein-10 from *Theobroma cacao*. *Genet. Mol. Res.* 12, 4855–4868. doi: 10.4238/2013.October.22.5
- Thakur, M., and Udayashankar, A. C. (2019). “Lipoxygenases and their function in plant innate mechanism,” in *Bioactive Molecules in Plant Defense*, eds S. Jogaiah and M. Abdelrahman (Cham: Springer International Publishing), 133–143. doi: 10.1007/978-3-030-27165-7_8
- Ueeda, M., Kubota, M., and Nishi, K. (2005). Contribution of jasmonic acid to resistance against Phytophthora blight in *Capsicum annuum* cv. SCM334. *Physiol. Mol. Plant Pathol.* 67, 149–154. doi: 10.1016/j.pmp.2005.12.002
- Valcu, C.-M., Junqueira, M., Shevchenko, A., and Schlink, K. (2009). Comparative proteomic analysis of responses to pathogen infection and wounding in *Fagus sylvatica*. *J. Proteome Res.* 8, 4077–4091. doi: 10.1021/pr900456c
- Vasyukova, N. I., and Ozeretskovskaya, O. L. (2009). Jasmonate-dependent defense signaling in plant tissues. *Russ. J. Plant Physiol.* 56, 581–590. doi: 10.1134/S102144370905001X
- Verli, H. (2014). (Org.) “Biologia de sistemas,” in *Bioinformática da Biologia à Flexibilidade Molecular, 1st Edn.* (Sociedade Brasileira de Bioquímica e Biologia Molecular-SBBq), 282. Available online at: <https://www.ufrgs.br/bioinfo/ebook/> (accessed July 7, 2018).
- Veronesi, C., Rickauer, M., Fournier, J., Pouenat, M. L., and Esquerre-Tugay, M. T. (1996). Lipoxygenase gene expression in the tobacco–*Phytophthora parasitica* interaction. *Plant Physiol.* 112, 997–1004. doi: 10.1104/pp.112.3.997
- Villela-Dias, C., Camillo, L. R., de Oliveira, G. A. P., Sena, J. A. L., Santiago, A. S., de Sousa, S. T. P., et al. (2014). Nep1-like protein from *Moniliophthora perniciosa* induces a rapid proteome and metabolome reprogramming in cells of *Nicotiana benthamiana*. *Physiol. Plant.* 150, 1–17. doi: 10.1111/ppl.12061
- Xu, Y.-H., Liu, R., Yan, L., Liu, Z.-Q., Jiang, S.-C., Shen, Y.-Y., et al. (2012). Light-harvesting chlorophyll a/b-binding proteins are required for stomatal response to abscisic acid in *Arabidopsis*. *J. Exp. Bot.* 63, 1095–1106. doi: 10.1093/jxb/err315
- Yamauchi, Y., Hasegawa, A., Mizutani, M., and Sugimoto, Y. (2012). Chloroplastic NADPH-dependent alkenal/one oxidoreductase contributes to the detoxification of reactive carbonyls produced under oxidative stress. *FEBS Lett.* 586, 1208–1213. doi: 10.1016/j.febslet.2012.03.013
- Yamauchi, Y., Hasegawa, A., Taninaka, A., Mizutani, M., and Sugimoto, Y. (2011). NADPH-dependent reductases involved in the detoxification of reactive carbonyls in plants. *J. Biol. Chem.* 286, 6999–7009. doi: 10.1074/jbc.M110.202226
- Zhang, C., Liu, L., Wang, X., Vossen, J., Li, G., Li, T., et al. (2014). The Ph-3 gene from *Solanum pimpinellifolium* encodes CC-NBS-LRR protein conferring resistance to *Phytophthora infestans*. *Theor. Appl. Genet.* 127, 1353–1364. doi: 10.1007/s00122-014-2303-1
- Zhang, D., and Motilal, L. (2016). “Origin, dispersal, and current global distribution of cacao genetic diversity,” in *Cacao Diseases* (Cham: Springer International Publishing), 3–31. doi: 10.1007/978-3-319-24789-2_1
- Zhang, X.-F., Jiang, T., Wu, Z., Du, S.-Y., Yu, Y.-T., Jiang, S.-C., et al. (2013). Cochaperonin CPN20 negatively regulates abscisic acid signaling in *Arabidopsis*. *Plant Mol. Biol.* 83, 205–218. doi: 10.1007/s11103-013-0082-8

Conflict of Interest: The authors declare that the research was conducted in the absence of any commercial or financial relationships that could be construed as a potential conflict of interest.

Publisher’s Note: All claims expressed in this article are solely those of the authors and do not necessarily represent those of their affiliated organizations, or those of the publisher, the editors and the reviewers. Any product that may be evaluated in this article, or claim that may be made by its manufacturer, is not guaranteed or endorsed by the publisher.

Copyright © 2022 Rego, Mora-Ocampo, Pirovani, Luz and Corrêa. This is an open-access article distributed under the terms of the Creative Commons Attribution License (CC BY). The use, distribution or reproduction in other forums is permitted, provided the original author(s) and the copyright owner(s) are credited and that the original publication in this journal is cited, in accordance with accepted academic practice. No use, distribution or reproduction is permitted which does not comply with these terms.